



This is a repository copy of *Evaluation of a Kinematically-Driven Finite Element Footstrike Model*.

White Rose Research Online URL for this paper:  
<http://eprints.whiterose.ac.uk/94871/>

Version: Accepted Version

---

**Article:**

Hannah, I., Harland, A., Price, D. et al. (2 more authors) (2016) Evaluation of a Kinematically-Driven Finite Element Footstrike Model. *Journal of Applied Biomechanics*, 32 (3). pp. 301-305. ISSN 1065-8483

<https://doi.org/10.1123/jab.2015-0002>

---

**Reuse**

Unless indicated otherwise, fulltext items are protected by copyright with all rights reserved. The copyright exception in section 29 of the Copyright, Designs and Patents Act 1988 allows the making of a single copy solely for the purpose of non-commercial research or private study within the limits of fair dealing. The publisher or other rights-holder may allow further reproduction and re-use of this version - refer to the White Rose Research Online record for this item. Where records identify the publisher as the copyright holder, users can verify any specific terms of use on the publisher's website.

**Takedown**

If you consider content in White Rose Research Online to be in breach of UK law, please notify us by emailing [eprints@whiterose.ac.uk](mailto:eprints@whiterose.ac.uk) including the URL of the record and the reason for the withdrawal request.



[eprints@whiterose.ac.uk](mailto:eprints@whiterose.ac.uk)  
<https://eprints.whiterose.ac.uk/>

1 November 13, 2015

2 JAB.2015-0002.R2

3

4 **Evaluation of a Kinematically Driven Finite Element Footstrike Model**

5

6 Iain Hannah,<sup>1,2</sup> Andy Harland,<sup>1</sup> Dan Price,<sup>3</sup> Heiko Schlarb,<sup>3</sup> and Tim Lucas<sup>3</sup>

7 <sup>1</sup>Sports Technology Institute, Loughborough University, Loughborough, UK;

8 <sup>2</sup>INSIGNEO Institute for *in silico* Medicine, University of Sheffield, Sheffield, UK;

9 <sup>3</sup>adidas AG, Herzogenaurach, Bavaria, Germany

10

11 **Funding:** *adidas AG supported this study with funding and were involved in the collection of*  
12 *biomechanical data.*

13 **Conflict of Interest Disclosure:** *None.*

14 **Correspondence Address:** Iain Hannah. *Tel.: +44 (0) 7745 833 099, fax: +44 (0)1509 564 820.*

15 *E-mail address: i.hannah@sheffield.ac.uk*

16 **Running Title:** *A Kinematically Driven FE Footstrike Model*

17 **Abstract (199 words)**

18 A dynamic finite element model of a shod running footstrike was developed and driven with six  
19 degree of freedom foot segment kinematics determined from a motion capture running trial.  
20 Quadratic tetrahedral elements were used to mesh the footwear components with material models  
21 determined from appropriate mechanical tests. Model outputs were compared to experimental  
22 high speed video (HSV) footage, vertical ground reaction force (GRF) and centre of pressure  
23 (COP) excursion to determine whether such an approach is appropriate for the development of  
24 athletic footwear.

25 Although unquantified, good visual agreement to the HSV footage was observed but significant  
26 discrepancies were found between the model and experimental GRF and COP readings (9% and  
27 61% of model readings outside of the mean experimental reading  $\pm 2$  standard deviations  
28 respectively). Model output was also found to be highly sensitive to input kinematics with a  
29 120% increase in maximum GRF observed when translating the force platform 2 mm vertically.

30 Whilst representing an alternative approach to existing dynamic finite elements footstrike  
31 models, loading highly representative of an experimental trial was not found to be achievable  
32 when employing exclusively kinematic boundary conditions. This significantly limits the  
33 usefulness of employing such an approach in the footwear development process.

34

35 Keywords: finite element analysis, athletic footwear, running, kinematics, ground reaction  
36 force

37 **Word Count:** 1995

38

## Introduction

39 In order to satisfy increasing consumer demand for enhanced performance, athletic  
40 footwear brands invest significantly in the design of novel footwear technologies. Mechanical,  
41 biomechanical and user wear trials are all typically employed in an iterative design process but  
42 this approach is both time consuming and expensive.<sup>1</sup> As a result, several leading brands have  
43 begun to adopt computer aided engineering (CAE) techniques in order to minimise costs and  
44 reduce development times.<sup>2,3</sup>

45 The potential utility of a rigid-body-dynamics based foot-footwear-floor contact model  
46 was reported by Wright et al.<sup>4</sup> and has the potential to allow the mechanical performance of  
47 prospective footwear designs to be evaluated in a virtual environment, avoiding the variation  
48 inherent in human testing<sup>5</sup> and reducing the need for physical prototyping. A number of finite  
49 element (FE) footstrike models have been reported but these studies have been limited to two  
50 dimensional analyses,<sup>6,7</sup> with quasi-static loading<sup>8</sup> and largely simplified boundary conditions  
51 applied.<sup>9,10</sup>

52 In order to provide an accurate prediction of an item of footwear's response to loading, a  
53 footstrike model would have to contain accurate footwear geometries, an appropriate mesh and,  
54 sophisticated material models characteristic of those used in modern athletic footwear. Most  
55 importantly, the boundary conditions used in any model must be representative of the complex,  
56 multiaxial and dynamic loading applied to the footwear during a footstrike.

57 This paper presents the first dynamic FE model of a shod footstrike to employ kinematic  
58 boundary conditions determined directly from the motion capture of experimental running trials.  
59 The sensitivity of the model to input kinematics is evaluated with its ability to apply  
60 biomechanically representative load conditions investigated through comparison of the modelled

61 and experimental loading conditions. This paper thus aims to answer whether it would be  
62 appropriate to adopt such an approach in the development of athletic footwear.

63

## 64 **Methods**

### 65 **Determining Boundary Conditions**

66 Boundary conditions typical of a shod heel-toe running footstrike were determined from  
67 six biomechanical overground motion capture trials performed by a healthy, male subject  
68 (age: 24 years, height: 1.76 m, mass: 69 kg). The participant gave informed ethical consent to  
69 take part in the study, which was conducted in accordance with the protocol approved by the  
70 [Name deleted to maintain the integrity of the review process] Ethical Advisory Committee.

71 Ten spherical retroreflective markers were attached to the shod left foot of the subject in  
72 accordance with the Heidelberg Foot Measurement Method.<sup>11</sup> The subject wore a simple athletic  
73 shoe manufactured specifically for the test which consisted of an ethylene-vinyl acetate (EVA)  
74 midsole, a blown rubber outsole, and simple laced upper. Running speed was controlled to be  
75  $4.0 \pm 0.1 \text{ m}\cdot\text{s}^{-1}$  with reflective laser timing gates.

76 The 3-D trajectories of each marker were recorded with a network of 12 infrared cameras  
77 (Vicon, UK) sampling at 200 Hz. Vertical ground reaction force (GRF) was measured at a  
78 sample rate of 1000 Hz with a piezoelectric force platform (Kistler, Winterthur, Switzerland)  
79 with synchronised high speed video (HSV) footage obtained with dual cameras (Photron, Tokyo,  
80 Japan).

81 Similar to Carson et al.,<sup>12</sup> the biomechanical model employed consisted of three rigid  
82 segments: a rearfoot calcaneal segment, a metatarsal segment including the five metatarsal rays

83 and a forefoot segment encompassing all fourteen phalangeal bones (Fig. 1). The foot model was  
84 built in Visual3D (C-Motion, Germantown, MD) from a static standing trial performed by the  
85 subject. The 3-D translations and rotations of each segment were determined by subsequently  
86 performing an inverse kinematics analysis of each dynamic trial.

87 In accordance with ISB guidelines,<sup>13</sup> rotation amplitudes for each functional foot segment  
88 were calculated about the laboratory origin with a Cardan sequence of X (M-L), Y (A-P),  
89 Z (dorsoventral). The six degree of freedom kinematic data of each segment were then filtered  
90 with a fourth order low-pass bidirectional Butterworth filter with a cut-off frequency of 8 Hz.

91 When fitting the static model to each dynamic trial, typical segment residual values<sup>14</sup> of  
92 2 - 4 mm were obtained. The trial with the lowest aggregate segment residual value  
93 (calcaneus: 2.0 mm, metatarsals: 2.3 mm, phalanges: 2.2 mm) was selected for finite element  
94 modelling.

### 95 **Finite Element Modelling**

96 To allow for the positioning of the footwear midsole and outsole geometries in the  
97 laboratory coordinate system, the three dimensional geometry of the lasted shoe and its attached  
98 markers was captured with an ATOS I 800 Digitizer stereo fringe projection scanner (GOM  
99 mbH, Braunschweig, Germany). The pose of the scanned geometry was then determined by  
100 rigidly registering the ten scanned markers with the marker locations measured from the last  
101 frame of the biomechanical trial captured before contact with the force platform. The average  
102 registration residual was 4.0 mm. Surface-based CAD geometries of the midsole and outsole  
103 obtained from manufacturing tooling profiles were subsequently aligned to the scan geometry  
104 and exported for meshing.



128 modified quadratic tetrahedral elements as they have been shown to perform consistently well in  
129 a range of foot and footwear simulations.<sup>15</sup> The laboratory force platform was modelled with  
130 rigid, shell elements.

131 Petre et al.<sup>16</sup> called into question the results of several studies which determined the  
132 material parameters of FE elastomeric foams models from single modes of testing. The stress-  
133 strain response of EVA was thus characterised for multiple modes of deformation: uniaxial  
134 tension, simple compression, and planar shear (5565 universal testing machine, Instron,  
135 Norwood, MA). Using Abaqus 6.12 (Dassault Systèmes, Vélizy-Villacoublay, France) it was  
136 found that the most appropriate representation of the EVA midsole's response under loading  
137 could be achieved with a first-order hyperfoam strain energy density function.<sup>17</sup>

138 Similarly, material parameters for the blown rubber used in the outsole were determined  
139 from uniaxial tension and simple compression tests. The material was found to be best  
140 represented with a third-order hyperelastic strain energy function.<sup>17</sup> Near incompressible material  
141 behaviour was ensured by defining a Poisson's ratio of 0.475.

142 Finally, an incompressible second-order hyperelastic material model was used to  
143 characterise the behaviour of the homogenous foot geometry with material parameters reverse  
144 engineered to provide sufficient constraint at the midfoot and metatarsophalangeal joints  
145 included in the model. Materials parameters are not reported as they have been developed in a  
146 commercially sensitive environment.

147 The model outputs of interest were found to be uninfluenced by the definition of  
148 tangential contact. As such, frictionless penalty contact was defined between the rigid force  
149 platform and all deformable bodies in the analysis. Adjacent foot and footwear surfaces were  
150 also constrained with kinematic ties. The analysis was submitted to the Abaqus/Explicit solver.



151 Validation of the modelling approach was attempted by comparing the model GRF and  
152 COP outputs to the experimental trials from which the applied boundary conditions were  
153 determined. An acceptable result was considered to fall within two standard deviations (sd) of  
154 the mean experimental value (n=6) and could thus be considered representative of the modelled  
155 movement task.<sup>18</sup>

156 The sensitivity of model output to the applied kinematics was investigated by performing  
157 two further analyses in which the position of the force platform instance was translated vertically  
158  $\pm 2$  mm. A translation of 2 mm was selected to correspond with the minimum segment residual  
159 value observed.

## 160 **Results**

161  
162 [Figure 2 near here]

163  
164 Whilst unquantified, good visual agreement was seen between model field output and  
165 high speed video footage of the corresponding biomechanical trial (Fig. 2). This is however to  
166 be expected for a kinematically driven model.

167  
168 [Figure 3 near here]

169  
170 Model GRF output displayed distinct impact and propulsive force peaks but overall  
171 agreement to the experimental trial was poor with only 9% of model outputs falling within two  
172 standard deviations (sd) of the mean experimental value (Fig. 3). The simulated impact force  
173 peak was 26% lower and the impact force peak 14% higher than during experimental testing.

174 This indicates that the discrepancy between simulated and experimental loading profiles is not  
175 due to a systematic error. The overall root-mean-square (RMS) deviation was 143 N with the  
176 total duration of the stance phase also reduced by 0.034 s relative to the modelled experimental  
177 trial.

178

179 [Figure 4 near here]

180

181 Agreement to experimental COP excursion was also found to be poor with only 45%  
182 (A-P) and 78% (M-L) of model outputs registering within two sd of the experimental means.  
183 Relative to the experimental trial modelled, RMS deviations of 13.7 mm (A-P) and 8.7 mm  
184 (M-L) were observed with the maximum residual found to be 24.7 mm. The first 0.01 s of the  
185 footstrike was omitted from the analysis as experimental COP measurement can be unreliable  
186 when the vertical GRF is small.<sup>19</sup>

187 Finally, the modelling methodology was found to be highly sensitive to the applied  
188 kinematics with a 2 mm adjustment in the position of the force platform resulting in a maximum  
189 change in model GRF of 2.3 kN. A translation of +2 mm along the vertical axis was found to  
190 increase the impact force peak by 52% and the propulsive force peak by 120%. Similarly,  
191 translating the force platform -2 mm was found to reduce the impact and propulsive force peaks  
192 by 34% and 44% respectively.

193

## 194 Discussion

195 The utility of a kinematically driven footstrike model has been evaluated in this paper by  
196 determining if the reported model was capable of applying simulated loading representative of a

197 shod footstrike. The approach of employing experimentally measured kinematic boundary  
198 conditions is novel and agreement to HSV footage was good but only 9% of model GRF outputs  
199 and 61% of COP excursion readings fell within two sd of the experimental means, thus failing  
200 the validation criteria. This indicates that the proposed methodology cannot apply loading  
201 representative of a running footstrike.

202 This can be explained by the demonstrated sensitivity of the model to the defined  
203 boundary conditions (Fig. 5) and the uncertainty inherent in their measurement. The registration  
204 technique employed to position the footwear relative to the force platform resulted in an average  
205 residual of 4 mm at each marker location. Segment residual values of 2 – 4 mm were calculated  
206 when fitting the static foot model to a dynamic trial and movement artefact of the in-shoe foot  
207 segments relative to the shoe-mounted markers<sup>20</sup> was entirely unaccounted for. By comparison,  
208 adjusting the position of the force platform by only 2 mm increased the applied loads by up to  
209 120%.

210 It can thus be concluded that an FE footstrike model driven exclusively by foot segment  
211 kinematics, as described in this study, cannot accurately represent the complex, dynamic loading  
212 characteristics of a human footstrike. Without greater confidence in the 3-D kinematics of the  
213 foot segments, a highly accurate representation of experimental loading patterns will not be  
214 achievable. This greatly limits the value of such an approach when evaluating prospective  
215 footwear designs and it is therefore suggested that an alternative, force driven approach is  
216 pursued.

217

## References

- 218 1. Cheung JTM, Yu J, Wong DW-C, Zhang M. Current methods in computer-aided  
219 engineering for footwear design. *Footwear Sci.* 2009;1(1):31-46.  
220 doi:10.1080/19424280903002323.
- 221 2. Azariadis P. Virtual shoe test bed: a computer aided engineering tool for supporting shoe  
222 design. *Comput Aided Des Appl.* 2007;4(741-750).  
223 doi:10.1080/16864360.2007.10738507.
- 224 3. Covill D, Guan ZW, Bailey M, Raval H. Development of thermal models of footwear  
225 using finite element analysis. *Proc Inst Mech Eng H.* 2011;225(3):268-81.
- 226 4. Wright IC, Neptune RR, van den Bogert AJ, Nigg BM. The influence of foot positioning  
227 on ankle sprains. *J Biomech.* 2000;33(5):513-519. doi:http://dx.doi.org/10.1016/S0021-  
228 9290(99)00218-3.
- 229 5. Erdemir A, Saucerman JJ, Lemmon D, et al. Local plantar pressure relief in therapeutic  
230 footwear: design guidelines from finite element models. *J Biomech.* 2005;38(9):1798-  
231 1806. doi:10.1016/j.jbiomech.2004.09.009.
- 232 6. Halloran JP, Ackermann M, Erdemir A, van den Bogert AJ. Concurrent musculoskeletal  
233 dynamics and finite element analysis predicts altered gait patterns to reduce foot tissue  
234 loading. *J Biomech.* 2010;43(14):2810-2815. doi:10.1016/j.jbiomech.2010.05.036.
- 235 7. Verdejo R, Mills NJ. Heel-shoe interactions and the durability of EVA foam running-shoe  
236 midsoles. *J Biomech.* 2004;37(9):1379-1386. doi:10.1016/j.jbiomech.2003.12.022.
- 237 8. Cheung JTM, Bouchet B, Zhang M, Nigg BM, Frederick EC, Yang SW. A 3D finite  
238 element simulation of foot-shoe interface. In: *8th Footwear Biomechanics Symposium.*  
239 Taipei; 2007:45-46.
- 240 9. Even-Tzur N, Weisz E, Hirsch-Falk Y, Gefen A. Role of EVA viscoelastic properties in  
241 the protective performance of a sport shoe: Computational studies. *Biomed Mater Eng.*  
242 2006;16:289-299.
- 243 10. Goske S, Erdemir A, Petre MT, Budhabhatti S, Cavanagh PR. Reduction of plantar heel  
244 pressures: Insole design using finite element analysis. *J Biomech.* 2006;39(13):2363-2370.  
245 doi:10.1016/j.jbiomech.2005.08.006.
- 246 11. Simon J, Doederlein L, McIntosh AS, Metaxiotis D, Bock HG, Wolf SI. The Heidelberg  
247 foot measurement method: Development, description and assessment. *Gait Posture.*  
248 2006;23(4):411-424. doi:10.1016/j.gaitpost.2005.07.003.
- 249 12. Carson MC, Harrington ME, Thompson N, O'Connor JJ, Theologis TN. Kinematic  
250 analysis of a multi-segment foot model for research and clinical applications: a

- 251 repeatability analysis. *J Biomech.* 2001;34(10):1299-1307. doi:10.1016/s0021-  
252 9290(01)00101-4.
- 253 13. Wu G, Siegler S, Allard P, et al. ISB recommendation on definitions of joint coordinate  
254 system of various joints for the reporting of human joint motion--part I: ankle, hip, and  
255 spine. *J Biomech.* 2002;35(4):543-548. doi:10.1016/s0021-9290(01)00222-6.
- 256 14. Spoor CW, Veldpaus FE. Rigid body motion calculated from spatial co-ordinates of  
257 markers. *J Biomech.* 1980;13(4):391-393. doi:10.1016/0021-9290(80)90020-2.
- 258 15. Tadepalli SC, Erdemir A, Cavanagh PR. Comparison of hexahedral and tetrahedral  
259 elements in finite element analysis of the foot and footwear. *J Biomech.*  
260 2011;44(12):2337-2343. doi:http://dx.doi.org/10.1016/j.jbiomech.2011.05.006.
- 261 16. Petre MT, Erdemir A, Cavanagh PR. Determination of elastomeric foam parameters for  
262 simulations of complex loading. *Comput Methods Biomech Biomed Engin.* 2006;9(4):231-  
263 242.
- 264 17. Abaqus. *Abaqus Theory Manual.* Providence, RI: Dassault Systèmes; 2012.
- 265 18. Hicks JL, Uchida TK, Seth A, Rajagopal A, Delp S. Is my model good enough? Best  
266 practices for verification and validation of musculoskeletal models and simulations of  
267 human movement. *J Biomech Eng.* 2014;137(2):020905. doi:10.1115/1.4029304.
- 268 19. Kwon YH. Center of pressure (GRF application point). 1998. Available at:  
269 <http://www.kwon3d.com/theory/grf/cop.html>. Accessed February 8, 2012.
- 270 20. Sinclair J, Taylor PJ, Hebron J, Chockalingam N. Differences in multi-segment foot  
271 kinematics measured using skin and shoe mounted markers. *Foot Ankle Online J.* 2014.
- 272

273

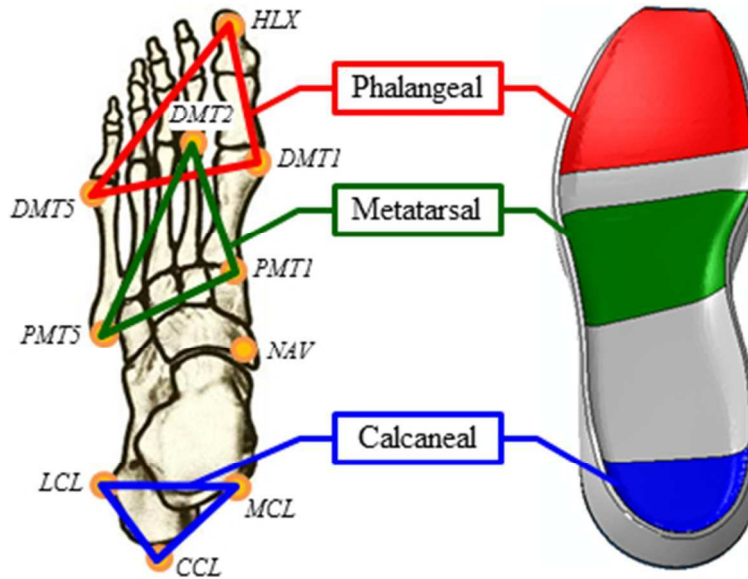
**Figure Captions**

274 **Figure 1** - Three segment foot model encompassing calcaneal, metatarsal and phalangeal  
275 segments and footwear instances with corresponding rigid foot segment plates.

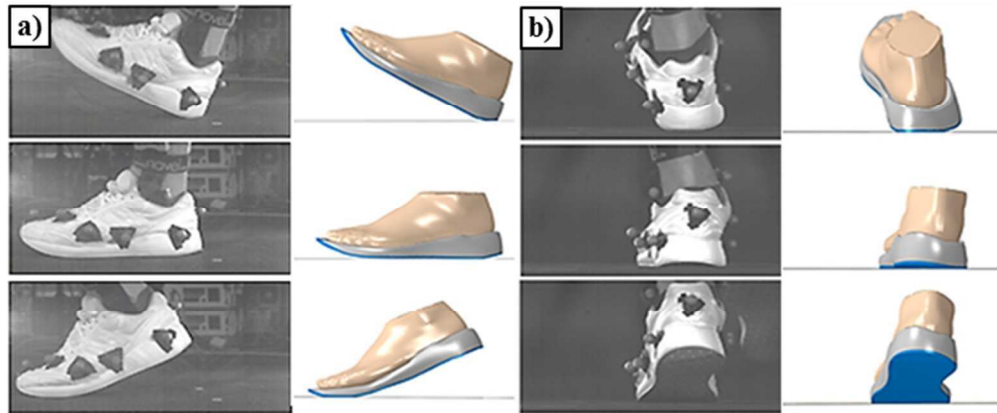
276 **Figure 2** - Visual comparison of model field output to experimental HSV footage at heelstrike,  
277 midstance and push-off. (a) Lateral view. (b) Posterior view.

278 **Figure 3** - Comparison of modelled and experimental vertical ground reaction forces with  
279 impact and propulsive force peaks shown.

280 **Figure 4** - Comparison of simulated and experimental COP excursion (a) Anteroposterior axis. (b)  
281 Mediolateral axis.



Three segment foot model encompassing calcaneal, metatarsal and phalangeal segments and footwear instances with corresponding rigid foot segment plates.  
102x75mm (96 x 96 DPI)

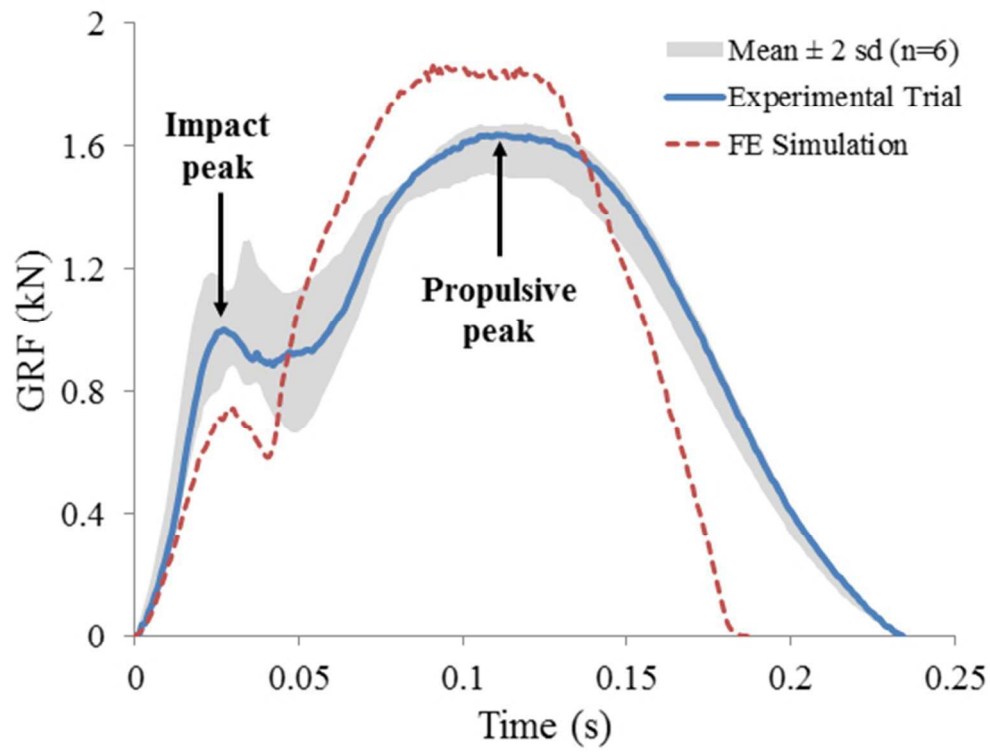


Visual comparison of model field output to experimental HSV footage at heelstrike, midstance and push-off.

(a) Lateral view. (b) Posterior view.

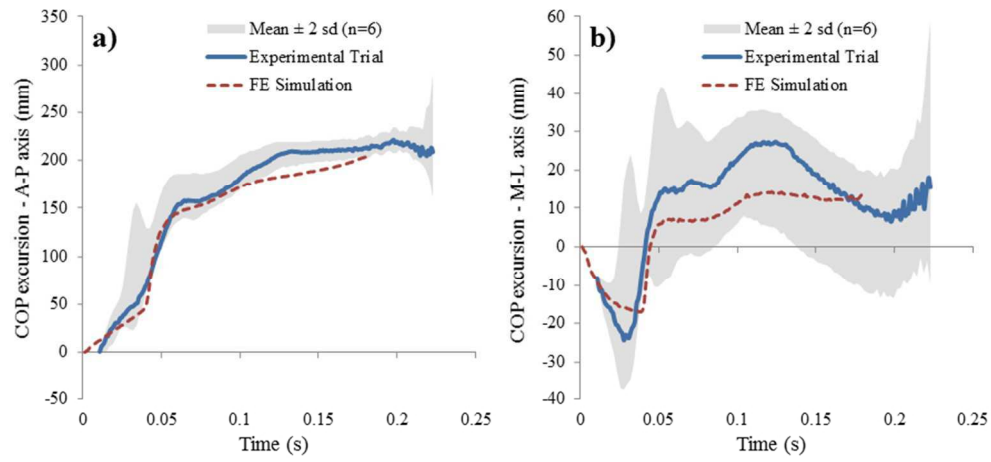
185x76mm (96 x 96 DPI)





Comparison of simulated and experimental vertical ground reaction forces with impact and propulsive force peaks shown.

159x119mm (96 x 96 DPI)



Comparison of simulated and experimental COP excursion (a) Anteroposterior axis. (b) Mediolateral axis.  
238x111mm (96 x 96 DPI)